

MAX-PLANCK-INSTITUT FÜR PLASMAPHYSIK
GARCHING BEI MÜNCHEN

Axisymmetric MHD Stability of Sharp-boundary Tokamaks

E. Rebhan, A. Salat

IPP 6/150

September 1976

Die nachstehende Arbeit wurde im Rahmen des Vertrages zwischen dem Max-Planck-Institut für Plasmaphysik und der Europäischen Atomgemeinschaft über die Zusammenarbeit auf dem Gebiete der Plasmaphysik durchgeführt.

September 1976 (in English)

Abstract

For a sharp-boundary, constant-pressure plasma model of axisymmetric equilibria the MHD stability problem of axisymmetric perturbations is solved by analytic reduction to a one-dimensional problem on the boundary and subsequent numerical treatment, using the energy principle. The stability boundaries are determined for arbitrary aspect ratio, arbitrary β_p and elliptical, triangular and rectangular plasma cross-sections, wall stabilization not being taken into account. It is found that axisymmetric stability strongly depends on the plasma shape and is almost independent of the safety factor q .

1. Introduction

The sharp-boundary model - plasma with constant pressure and surface currents surrounded by vacuum [1] , [2] - is, from a mathematical viewpoint, especially suitable for the study of ideal MHD stability owing to its relative simplicity. Although many of the interesting subtleties of more realistic plasma models are certainly missing in this model, the most dangerous and important ideal MHD instabilities (those which push the whole plasma towards the outer wall) are present and are believed to be fairly well described by it. Besides its application to stellarators and related configurations, for which cases special complications arise with other models, this model has also been extensively used for the study of axisymmetric devices such as tokamaks.

Concerning axisymmetric sharp-boundary equilibria the stability analysis for nonaxisymmetric perturbations has a long history. A straight approximation with circular cross-section and toroidal topology was investigated in Ref. [3]. In Ref. [4] a general outline of the method in toroidal geometry was presented and applied to plasmas with circular cross-sections in the limit of infinite aspect ratio. Finite aspect ratio but only circular cross-sections (i.e. as far as explicit results are concerned) have been studied in [5] , [6] , while finite aspect ratio and rather arbitrary cross-sections were considered in [7] .

Axisymmetric perturbations have long been wallflowers in the stability

theory of axisymmetric equilibria (step profile model and others), the reason probably being twofold. Firstly, the use of material plasma limiters in experiments has either prevented or concealed the appearance of external axisymmetric perturbations, while sufficient stability criteria [8] show that internal axisymmetric perturbations are stable in many cases of practical interest. Secondly, experimentalists have long been shy of departing appreciably from circular plasma cross-sections. According to the results of this paper, external axisymmetric instabilities have thus been avoided and, consequently, no pressing need to deal with axisymmetric perturbations emerged from the experiments.

Recently, the interest in plasma containment without material limiters and promising physical and technical features of plasmas with non-circular cross-sections have led to a growing interest in axisymmetric stability. Special simple perturbations such as rigid vertical shift [9 - 13] were considered as well as general axisymmetric perturbations in the limit of infinite aspect ratio and on the assumptions of usual tokamak ordering [14 , 15 , 16]. In [17] it was demonstrated for the sharp-boundary model that so-called slip instabilities, which are the most dangerous axisymmetric perturbations in the limit of infinite aspect ratio, are definitely stabilized by finite aspect ratio.

In this paper, for the sharp-boundary model with various shapes of the plasma cross-section the full axisymmetric stability problem of axisymmetric equilibria is solved using the energy principle, and thus a gap left in earlier investigations has been closed. As in Ref. [17], the external conductors necessary for confinement are assumed to be permeable to the perturbational field.

In Section 2 equilibrium relations are summarized. In Section 3 the plasma contribution to $\delta^2 W$ is minimized and combined with the surface and vacuum contributions. In Section 4 numerical results are presented.

2. Collection of equilibrium relations

We consider the same equilibria as in Ref. [17] and the following relations are copied from there (all quantities being dimensionless).

With the notations of Fig. 1 the plasma surfaces S considered are

$$F(R, \vartheta, z) = e^2(R-1)^2 + (1+\tau_3^2)z^2 - 2A\tau_3(R-1)z^2 - A^2\tau_4(R-1)^2z^2 = \frac{e^2}{A^2}, \quad (2.1)$$

where A = aspect ratio, e = elongation of cross-section, and τ_3 and τ_4 describe triangular and rectangular deformations. We consider only the cases $\tau_3 \neq 0, \tau_4 = 0$ and $\tau_4 \neq 0, \tau_3 = 0$. For

$\tau_3 = 0, \tau_4 = 1$ the cross-section is a rectangle; for $\tau_4 = 0, |\tau_3| = 1$ it is almost a triangle (two sharp angles are limiting a straight section in the z -direction). In Fig. 2 a selection of typical cross-sections is shown.

The magnetic fields \underline{B}_{pl} and \underline{B}_v inside and outside the plasma are given by

$$\underline{B}_{pl} = \frac{\Lambda_p}{R} \underline{e}_\phi, \quad \underline{B}_v = \frac{\Lambda_v}{R} \underline{e}_\phi + B \underline{t}, \quad (2.2)$$

where $\underline{t} = \underline{n} \times \underline{e}_\phi$, $\underline{n} = \nabla F / |\nabla F|$, $\underline{e}_\phi = R \nabla \phi$ and

$$B = \frac{1}{R} [1 + \beta_p (R^2 - 1)]^{1/2}. \quad (2.3)$$

Here $\beta_p = 2p / (B|_{R=1})^2$ and B is normalized by $B|_{R=1} = 1$

so that

$$p = \frac{\beta_p}{2}. \quad (2.4)$$

Λ_p and Λ_v are related by

$$\Lambda_p^2 - \Lambda_v^2 = 1 - \beta_p. \quad (2.5)$$

The equilibrium is limited by the condition

$$\beta_p \leq \beta_p^* = \frac{A^2}{2A - 1}. \quad (2.6)$$

The safety factor q on S is given by

$$q = \frac{\Lambda_v q_g}{A}, \quad q_g = \frac{A}{2\pi} \oint \frac{dl}{R^2 B}, \quad (2.7)$$

the line integration extending along S in the R, z plane. With the

definition $\beta = p / (p + \frac{1}{2} B_{pl}^2|_{R=1})$ we have

$$\beta = \frac{\beta_p}{1 + \frac{A^2 q^2}{q_g^2}}, \quad (2.8)$$

$$\beta_p \leq 1 + \frac{A^2 q^2}{q_g^2}. \quad (2.9)$$

Finally, for the stability calculation it is useful to introduce a parameter

α by

$$\alpha^2 = \frac{3\Lambda_p^2}{5p}, \quad (2.10)$$

which is related to q and β_p by

$$\alpha^2 = \frac{6}{5} \left[\frac{1}{\beta_p} \left(1 + A^2 \frac{q^2}{q_z^2} \right) - 1 \right] \quad (2.11)$$

according to eqs. (2.4) - (2.5) and (2.7).

3. Stability

For a plasma with constant pressure and surface currents according to

Ref. [18] $\delta^2 W$ is given by

$$\delta^2 W = \delta W_{pl} + \delta W_s + \delta W_v, \quad (3.1)$$

$$\delta W_{pl} = \frac{1}{2} \int_{pl} d\tau \left\{ c u r l^2 (\underline{\xi} \times \underline{B}_{pl}) + \frac{5}{3} (\nabla \cdot \underline{\xi})^2 \right\}, \quad (3.2)$$

$$\delta W_s = \frac{1}{2} \int_s d\sigma \left\{ (\underline{\xi} \cdot \underline{n}) \underline{n} \cdot \nabla \left(\frac{1}{2} \underline{B}_v^2 - \frac{1}{2} \underline{B}_{pl}^2 \right) \right\}, \quad (3.3)$$

$$\delta W_v = \frac{1}{2} \int_s d\sigma (\underline{B}_v \cdot \delta \underline{B}_v) (\underline{\xi} \cdot \underline{n}). \quad (3.4)$$

The surface integral representation of δW_v in eq.(3.4) is obtained

from the usual form by Gauss's theorem using the assumption of

completely permeable external conductors. Following the general

minimization procedure described in Ref. [17] , for $\underline{\xi}, \underline{\eta}$ given on S ,

$$\underline{\xi} \cdot \underline{n} = \xi_n , \quad (3.5)$$

we shall first minimize δW_{pl} and calculate $\delta W_S + \delta W_v$. Then, $\delta^2 W$ will be minimized with respect to ξ_n .

a) Minimization of δW_{pl} :

Introducing unit vectors \underline{e}_R and \underline{e}_z in the R and z -directions, we write

$$\underline{\xi} = \xi \underline{e}_R + \eta \underline{e}_z + \gamma \underline{e}_z . \quad (3.6)$$

For axisymmetric perturbations we have $\partial \xi / \partial \vartheta = 0$ and with this we obtain from eq. (3.2) using eqs. (2.2), (2.4) and (2.10)

$$\delta W_{pl} = \frac{5}{6} \pi \beta_p \int \left[R \left(\xi_R + \eta_z + \frac{\xi}{R} \right)^2 + \frac{\alpha^2}{R^2} \left(\xi_R + \eta_z - \frac{\xi}{R} \right)^2 \right] dR dz . \quad (3.7)$$

The subscripts at ξ and η mean partial differentiation with respect to R and z respectively. Variation with respect to ξ and η yields the Euler equations

$$\begin{aligned} \left(\xi_R + \eta_z \right)_R + \frac{R^2 - \alpha^2}{R^2 + \alpha^2} \left(\frac{\xi}{R} \right)_R &= 0 , \\ \left(\xi_R + \eta_z + \frac{R^2 - \alpha^2}{R^2 + \alpha^2} \cdot \frac{\xi}{R} \right)_z &= 0 , \end{aligned} \quad (3.8)$$

which have the solution

$$\begin{aligned} \xi &= \frac{(\alpha^2 + R^2)^2}{4\alpha^2} f' , \\ \eta &= \left[f + \frac{\alpha^2 + R^2}{\alpha^2} \left(\frac{\alpha^2 - R^2}{4R} - R \right) f' - \frac{(\alpha^2 + R^2)^2}{4\alpha^2} f'' \right] z + g . \end{aligned} \quad (3.9)$$

Here, f and g are arbitrary functions of R , and primes denote differentiation with respect to R . The prescription (3.6) on S amounts to a boundary condition for the Euler equation which allows the functions f and g to be determined. As in Ref. [17], we split ξ_n for this purpose into

$$\xi_n = \xi_n^s + \xi_n^a, \quad (3.10)$$

where $\xi_n^s|_{-z} = \xi_n^s|_z$ and $\xi_n^a|_{-z} = -\xi_n^a|_z$. With the representation $R = R(l)$, $z = z(l)$ of S ($l = \text{arc length}$ according to Fig. 1) $f(R)$ and $g(R)$ may be considered on S as function of l , and we have $\underline{n} \cdot \underline{e}_R = \dot{z}$, $\underline{n} \cdot \underline{e}_z = -\dot{R}$, where dots denote differentiation with respect to l . Splitting eq. (3.5) into its symmetric and antisymmetric components, with eqs. (3.9) we readily obtain

$$g = -\frac{\xi_n^a}{\dot{R}}, \quad (3.11)$$

$$\ddot{f} + \left(\frac{\dot{z}}{z} - \frac{\ddot{R}}{\dot{R}} - \frac{\alpha^2 - 5R^2}{\alpha^2 + R^2} \cdot \frac{\dot{R}}{R} \right) \dot{f} - \frac{4\alpha^2 \dot{R}^2}{(\alpha^2 + R^2)^2} f = \frac{4\alpha^2}{(\alpha^2 + R^2)^2} \frac{\dot{R}}{z} \xi_n^s. \quad (3.12)$$

- (1) On S , g is uniquely determined by eq. (3.11) as a function of l . Since for the plasma surfaces considered here (eq. (3.1)) l is a unique function of R for $z \geq 0$ and since both ξ_n^a and $\dot{R}(l)$ are antisymmetric functions, g is also uniquely determined as a function of R . It is shown in the

Appendix that by the differential equation (3.12) for $f(l)$ and by the condition that $f(l)$ is symmetric with respect to the $z=0$ plane the function $f(R)$ is uniquely determined as well, and that δW_{pl} assumes its minimum for the values ξ and η thus obtained.

Using the Euler equations (3.8), the expression (3.7) for δW_{pl} may be integrated by parts to yield the surface integral

$$\delta W_{pl} = \frac{5}{6} \pi \beta_P \oint \frac{R^2 + \alpha^2}{R} f \xi_n^s dl. \quad (3.13)$$

Note that there is only a contribution from ξ_n^s to the minimum of δW_{pl} .

b) Calculation of δW_S , δW_v and minimization of $\delta^2 W$

We now have to calculate δW_S and δW_v for given $\underline{\xi} \cdot \underline{n}$. Since in the treatment of slip motions the corresponding problem is formally identical, we may quote the results from Ref. [17]. With

$n_R = \underline{n} \cdot \underline{e}_R = \dot{z}$ eq. (4.16) of Ref. [17] reads

$$\delta W_S = \pi \oint dl [(\xi_n^s)^2 + (\xi_n^a)^2] \left(\frac{1 - \beta_P}{R^3} \dot{z} - \kappa B^2 \right) R, \quad (3.14)$$

where

$$\kappa = - \underline{n} \cdot (\underline{t} \cdot \nabla \underline{t}) \quad (3.15)$$

is the curvature of the poloidal field component in eq. (2.2).

Furthermore, from Section 4c) of Ref.[17] we summarize

$$\delta W_v = \delta W_v^s + \delta W_v^a, \quad (3.16)$$

$$\delta W_v^s = \pi \oint dl RB \xi_n^s y^s, \quad \delta W_v^a = \pi \oint dl RB \xi_n^a y^a,$$

where y^s and y^a are the symmetric and antisymmetric constituents of the quantity $y = \underline{t} \cdot \underline{\delta B}_v$.

y^s and y^a are both to be determined from an inhomogeneous integral equation of the form

$$y = \frac{1}{2\pi} \oint K(l, l') y' dl' + \frac{1}{2\pi} \oint L(l, l') \sigma' dl'. \quad (3.17)$$

Furthermore, y^s must satisfy a side condition:

$$\oint dl [R v y^s + RB \xi_n^s \underline{t} \cdot \text{curl } \underline{v}] = \sigma. \quad (3.18)$$

Since here we only want to summarize the structure of the problem, we do not repeat the lengthy expressions for $K(l, l')$, $L(l, l')$, σ , v and $\text{curl } \underline{v}$. The reader who is interested in the details is referred to Ref. [17].

According to eqs. (3.13), (3.14) and (3.16) $\delta^2 W$ has separated into contributions coming from ξ_n^s and ξ_n^a :

$$\delta^2 W = \delta W^s(\xi_n^s, \xi_n^s) + \delta W^a(\xi_n^a, \xi_n^a). \quad (3.19)$$

Since according to eq. (3.13) the plasma contribution in δW^a is zero, δW^a is identical with the corresponding expression for slip motions in Ref. [17]. Thus we have the result that for the most general axisymmetric perturbations which are antisymmetric with respect to the $z = 0$ plane the stability boundaries coincide with those obtained for antisymmetric slip motions.

Turning to δW^s , the remaining minimization problem with respect to ξ_m^s is essentially identical with the corresponding problem for slip motions and solved numerically. The only difference is that here for calculating the plasma contribution (3.13) the differential equation (3.12) must be solved. For the numerical treatment eq. (3.12) is converted into a finite system of linear equations by using the method of trigonometric interpolation in keeping with the methods used for solving eqs. (3.16) and (3.17) in Ref. [17] (see also Ref. [19]).

We conclude this section with the remark that in the two limiting cases A finite, $q \rightarrow \infty$ and q finite, $A \rightarrow \infty$ the stability boundaries for symmetric perturbations coincide with the corresponding slip motion boundaries as well. This follows from the fact that in both of these cases one has according to eq. (2.11) $\alpha^2 \rightarrow \infty$, and that slip motions are characterized by the vanishing of the expression in parentheses following α^2 in the integrand of eq. (3.7).

4. Numerical results^{†)}

We have seen in Sec. 3b that general axisymmetric perturbations have the same stability boundaries as slip motions quite generally when they are antisymmetric, and, for the special cases $q \rightarrow \infty$ and/or $A \rightarrow \infty$, also when they are symmetric. In Figs. 3a, b and 4a, b, the stability boundaries for general axisymmetric perturbations are shown for $q = 1$ and several values of A and β_p respectively, Figs. 3a and 4a representing triangular and Figs. 3b and 4b representing rectangular plasma cross-sections (see Fig. 2). The regions inside the plotted eye-shaped boundaries, which consist of two intersecting branches, correspond to stable plasma behaviour; outside there exist either antisymmetric or symmetric unstable perturbations or both. The upper branches of these stability boundaries (for clarity all branches are truncated at the intersecting points) are due to antisymmetric instabilities and hence also apply for slip motions. For plasmas whose shape parameters correspond to points above these branches the minimizing antisymmetric perturbations are unstable slip motions. Typical examples are presented in Ref. [17]. The lower branches of the boundaries are due to symmetric instabilities and pass slightly above the corresponding slip motion boundaries. However, the distance from these is so small that it is not visible on the scale chosen in Figs. 3a, b and 4a, b. The symmetric instabilities minimizing $\delta^2 W$ which occur below these branches were found to be almost slip motions, the difference being almost invisible, a result which

^{†)} The following results were partly reported at the 7th Europ. Conf. on Plasma Physics and Contr. Fusion [20]. Owing to a mistake the curves presented there deviate rather slightly from the corresponding corrected curves in this paper.

may not be concluded a priori from the nearness of the boundaries.

Because of this close resemblance the reader is again referred to Ref. [17] for details about these symmetric instabilities.

In order to see where the slight influence of q on axisymmetric stability becomes largest, we consider the stability boundaries in an e, β_p plane for several triangular and rectangular cross-sections in Figs. 5a and 5b. The stable region is between corresponding curves on the left and right; an upper limit of β_p is provided by inequality (2.9) owing to nonexistence of equilibrium above this limit. For $q \rightarrow \infty$ this limit is identical with the limit $\beta_p = \beta_p^*$ defined by eq. (2.6), and for $q = 1$ it is just not quite visibly below. While the boundaries for antisymmetric perturbations on the right are independent of q , the boundaries for symmetric perturbations on the left show a slight dependence on q which increases with increasing β_p . Only the two cases $q = 1$ and $q = \infty$ (slip motion limit) are plotted, the boundaries for intermediate q values being in between. In the very neighbourhood of the equilibrium limit the symmetric boundaries for $q = 1$ bend to the right and depart more markedly from the $q = \infty$ boundaries until they reach the equilibrium limit at the point indicated by an arrow.

In Fig. 6 the inset shows the stability boundaries for two different triangular cross-sections in an A, e plane. On the scale of this plot the q -dependence of the stability boundaries for symmetric perturbations is

invisible. It is made visible by the blow-up in Fig. 6 and is seen to increase slightly with decreasing A . For rectangular cross-sections equivalent results are obtained.

Owing to the Kruskal-Shafranow limit, the interesting range of q -values is limited by $q \gtrsim 1$ (see Ref. [7] for sharp boundary plasmas with non-circular cross-sections), and in our stability diagrams for all intermediate q values the stability boundaries run between the boundaries for $q = 1$ and $q = \infty$. Since these deviate from each other more markedly only for values of β_p which are so close to the equilibrium limit that they are uninteresting, we may summarize that, at least for the sharp boundary model, the influence of q on axisymmetric stability is practically negligible.

Recently interest in tokamak-like configurations with strongly elongated cross-sections (see, for example, [21]) has grown. We have therefore pursued the stability boundary for symmetric perturbations beyond its intersection with the boundary for antisymmetric perturbations up into the region of stronger elongation. For triangular cross-sections the result, a closed curve, is shown in Fig. 7. For rectangular cross-sections qualitatively equivalent results are obtained. Since the stable region for symmetric perturbations lies inside these closed curves, there exist both symmetric and antisymmetric instabilities beyond a critical elongation. Examples of those are given in Figs. 8a and 8b respectively, the

parameters being chosen to resemble the parameters of the Garching Belt Pinch experiment [22]. While in this experiment the anti-symmetric instability was observed, there was no experimental indication of the symmetric one which, on the time scale of the experiment, is probably suppressed by wall stabilization due to a cylindrical copper shell which confines the plasma in the radial direction. A different argument for not observing the symmetric mode may be derived from the following paragraph.

The occurrence of a symmetric instability beyond a critical elongation which is larger than 1 is maintained in the limit $A \rightarrow \infty$ and provides a stringent difference between the sharp boundary model and a smooth pressure constant current model of plasma in this limit. That is, for the latter it was shown in Ref. [15], assuming elliptical plasma cross-sections, that for $e > 1$ all symmetric perturbations (even poloidal mode number $m \gg 2$) are stable. Closer investigation, which was restricted to elliptical cross-sections, showed that it is the constant current model which behaves singularly in this respect and not the sharp boundary model. The reason is the following: owing to the constraint of incompressibility, obtained from minimizing $\delta^2 W$ for $A \rightarrow \infty$ on the assumptions of usual Tokamak ordering, the $m = 0$ mode, which is the only unstable symmetric mode for the constant current model, must vanish exactly, while it does not have to vanish for the sharp boundary model and for other smooth current distributions.

According to the foregoing it may be expected, that the occurrence, structure and growth rates of symmetric instabilities in highly elongated tokamaks will strongly depend on the current profile.

This section is concluded with a discussion of the stability limitations on β . For convenience only elliptical cross-sections are considered. Figure 9 shows the stability boundaries in an e, β plane obtained for $q = 1$. In the stable region, curves $\beta_p = \text{const}$ are drawn which are obtained from eq. (2.8). The curve far to the right determines the onset of symmetric instabilities beyond a critical elongation as discussed in the preceding paragraphs. In the lateral flanks of the stable region a lower limit of β appears, while in the left flank there is additionally an upper limit below $\beta = 1$. However, a comparison with Fig. 5a shows that the appearance of the upper limit is restricted to β_p values near the equilibrium limit. The dependence of the lower and upper β -limits on q is shown in Fig. 10 for a typical situation. Again, curves $\beta_p = \text{const}$ are drawn in the stable region.

5. Summary and conclusions

Investigating the sharp boundary model we have found that axisymmetric stability is, on the one hand, practically independent of q and, on the other, strongly sensitive to the plasma shape. This result is in rather strong contrast with the properties of non-axisymmetric stability, where

strong q -dependence is combined with the possibility of stabilizing any plasma with fixed β_p by sufficiently large q , regardless of its shape. Specifically, in the limit $A \rightarrow \infty$ all cross-sections, except for circles, are unstable with respect to axisymmetric perturbations. Only for small A do appreciable deviations from circular shape become possible, large values of β_p in addition being favourable.

For the sharp boundary model, the boundaries for axisymmetric stability may be approximated with practically sufficient accuracy by a slip motion analysis owing to their weak dependence on q . For plasmas with smooth pressure profiles such an analysis [23] implies an enormous simplification relative to the full axisymmetric problem, and from our results we would deduce that it yields a good approximation also in this case.

Wall stabilization, which was not considered in this paper, will certainly lead to an increase of the stable regions, as it does in the limit $A \rightarrow \infty$ (Ref. [14]). However, if the confinement times are long enough, the practical realization of wall stabilization by copper shells will only lead to a reduction of the growth rates and leave the stability boundaries unaltered. Concerning the question whether a limiter could stabilize an axisymmetric instability it appears possible that the plasma is pressed against the limiter by the instability and peeled off layer by layer.

Appendix

We shall first prove the existence of a unique solution of eq. (3.12).

For this purpose we write it in the form

$$\ddot{f} + a(l)\dot{f} + b(l)f = c(l)\xi_n^s. \quad (\text{A1})$$

According to its definition $f(l)$ must be symmetric with respect to the $z = 0$ plane, and, since for symmetric functions $\dot{f}(l) = 0$ at $z = \sigma$, we may restrict ourselves to the interval $0 \leq l \leq L$ between the two intersections of the boundary with $z = 0$ and consider the boundary value problem

$$\dot{f}(0) = \dot{f}(L) = 0. \quad (\text{A2})$$

By Taylor expansion about $l=0$ and $l=L$ it is readily seen that $a(l)$, $b(l)$ and $c(l)$ remain finite and continuous, so that the problem is regular.

Let us consider the homogeneous boundary value problem

$$\ddot{f} + a(l)\dot{f} + b(l)f = 0, \quad \dot{f}(0) = \dot{f}(L) = 0. \quad (\text{A3})$$

With

$$A(l) = \int_0^l a(l') dl' \quad (\text{A4})$$

the differential equation in (A3) may be written

$$e^{-A} (\dot{f} e^A)' = -bf.$$

With this it follows that for any solution which satisfies the first boundary condition $\dot{f}(0) = 0$ we have

$$\dot{f}(l) = \int_0^l g(l, l') f(l') dl', \quad (\text{A5})$$

where

$$g(l, l') = -b(l') e^{[A(l') - A(l)]} . \quad (A6)$$

Since $b(l) = -4\alpha^2 R^2 / (\alpha^2 + R^2)^2$, we have $g(l, 0) = g(l, L) = 0$ and $g(l, l') > 0$ for $0 < l' < L$ and therefore according to (A5) a solution with $\dot{f}(L) = 0$ is impossible. Thus, the homogeneous problem (A3) has no solution except for $f \equiv 0$, and according to a theorem in the theory of ordinary differential equations the inhomogeneous boundary value problem (A1), (A2) has a unique solution (see, for example, Ref. [24]). With this and eqs. (3.9) and (3.11) it is shown that the Euler equations (3.8) have a solution.

We may now prove that this solution provides a minimum of δW_{pl} .

Denoting the solution by $\underline{\xi}_0$, we consider an arbitrary $\underline{\xi}$ with

$$\underline{n} \cdot \underline{\xi} = \underline{n} \cdot \underline{\xi}_0 = \xi_n$$

and write

$$\underline{\xi} = \underline{\xi}_0 + \underline{\eta} .$$

Obviously, $\underline{\eta}$ must satisfy $\underline{\eta} \cdot \underline{n} = 0$. Using this and the fact that $\underline{\xi}_0$ satisfies the Euler equations (3.8), after integration by parts it is easily seen that

$$\delta W_{pl}(\underline{\xi}, \underline{\xi}) = \delta W_{pl}(\underline{\xi}_0, \underline{\xi}_0) + \delta W_{pl}(\underline{\eta}, \underline{\eta}) .$$

Since according to eq. (3.7) $\delta W_{pl}(\underline{\eta}, \underline{\eta})$ is positive definite,

our statement is proven.

References

- [1] Biermann L., Hain K., Jörgens K., Lüst R., Z. Naturforschg. 12a (1957) 826
- [2] Jörgens K., Z. Naturforschg. 13a (1958) 493
- [3] Shafranov V.D., Sovj. J. Atomic Energy 1 (1956) 709
Rosenbluth M., Proc. 3d Int. Conf. on Ion. Phen. in Gases,
(Venice 1957)
Taylor R.J., Proc. Phys. Soc. London B70 (1957) 1049
- [4] Lüst R., Suydam B.R., Richtmyer R.D., Rotenberg A., Levy D.,
Phys. Fluids 4 (1961), 891
- [5] Martensen E., Z. Naturforschg. 17a (1962) 733
- [6] Martensen E., Sengbusch K.V., Proc. 11th Intern. Congr. of
Applied Mechanics, (Munich, 1964) 1010
- [7] Freidberg J.P., Grossmann W., Phys. Fluids 18 (1975) 1494
- [8] Dobrott D., Chu M.S., Phys. Fluids 16 (1973) 1371
- [9] Okabayashi M., Sheffield G., Nuclear Fusion 14 (1974) 263
- [10] Rebhan E., Nucl. Fusion 15 (1975) 277
- [11] Lackner K., MacMahon A.B., Nucl. Fusion 14 (1974) 575
- [12] Mukhovatov V.S., Shafranov V.D., Nucl. Fusion 11 (1971) 605
- [13] Yoshikawa S., Phys. Fluids 7 (1964) 278

- [14] Laval G., Pellat R., Soulé J.S., *Phys. Fluids* 17 (1974) 835
- [15] Rutherford P.H., Princeton Report MATT-976 (1973)
- [16] Rosen M.D., *Phys. Fluids* 18 (1975) 482
- [17] Rebhan E., Salat A., IPP Report, 6/148 (1976)
- [18] Bernstein I.B., Frieman E.A., Kruskal M.B., Kulsrud R.M.,
Proc. Roy. Soc. A 244 (1958) 17
- [19] Martensen E., *Acta mathematica* 109 (1963) 75
- [20] Rebhan E., Salat A., Seventh Europ. Conf. on Contr. Fusion
and Plasma Physics (Lausanne 1975) Vol. II, p. 274
- [21] Schlüter J., 3d Top. Conf. on Pulsed High Beta Plasmas
(Culham 1975)
- [22] Gruber O., Wilhelm R., *Nucl. Fusion* 16 (1976) 243
- [23] Lackner K., Proc. 2nd Conf. on Comp. Phys. (Garching 1976)
C 4
- [24] Kamke E., Differentialgleichungen I., Akad. Verlagsges.,
Leipzig 1964, p. 231.

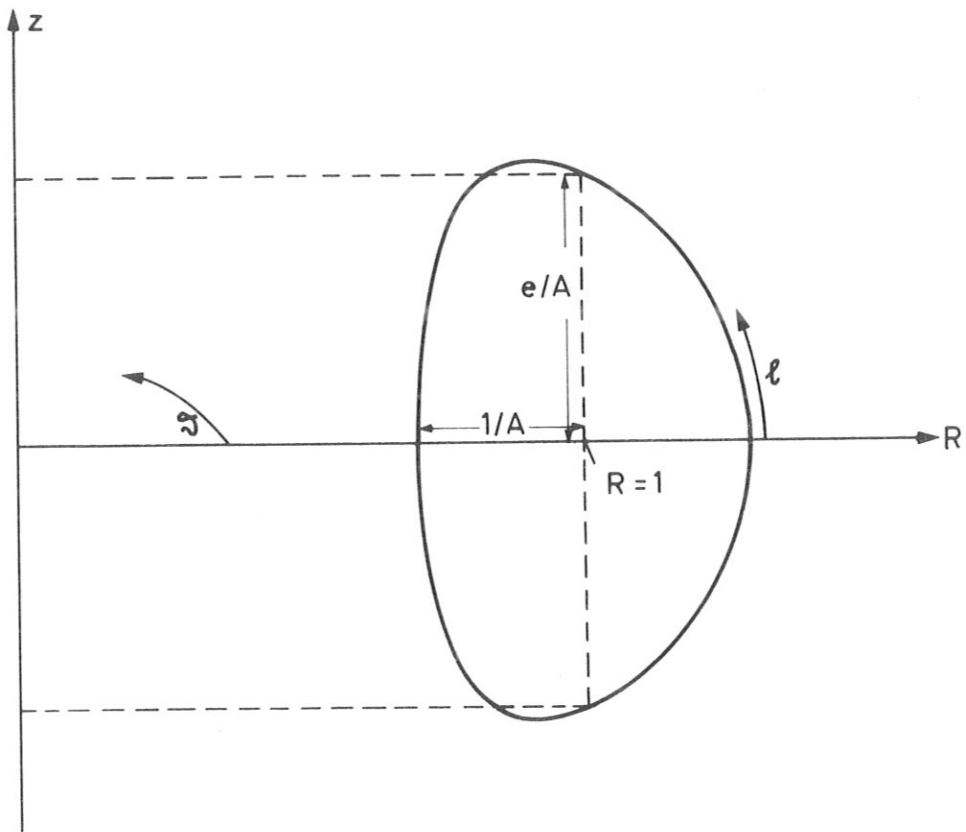


Fig. 1: Coordinate system

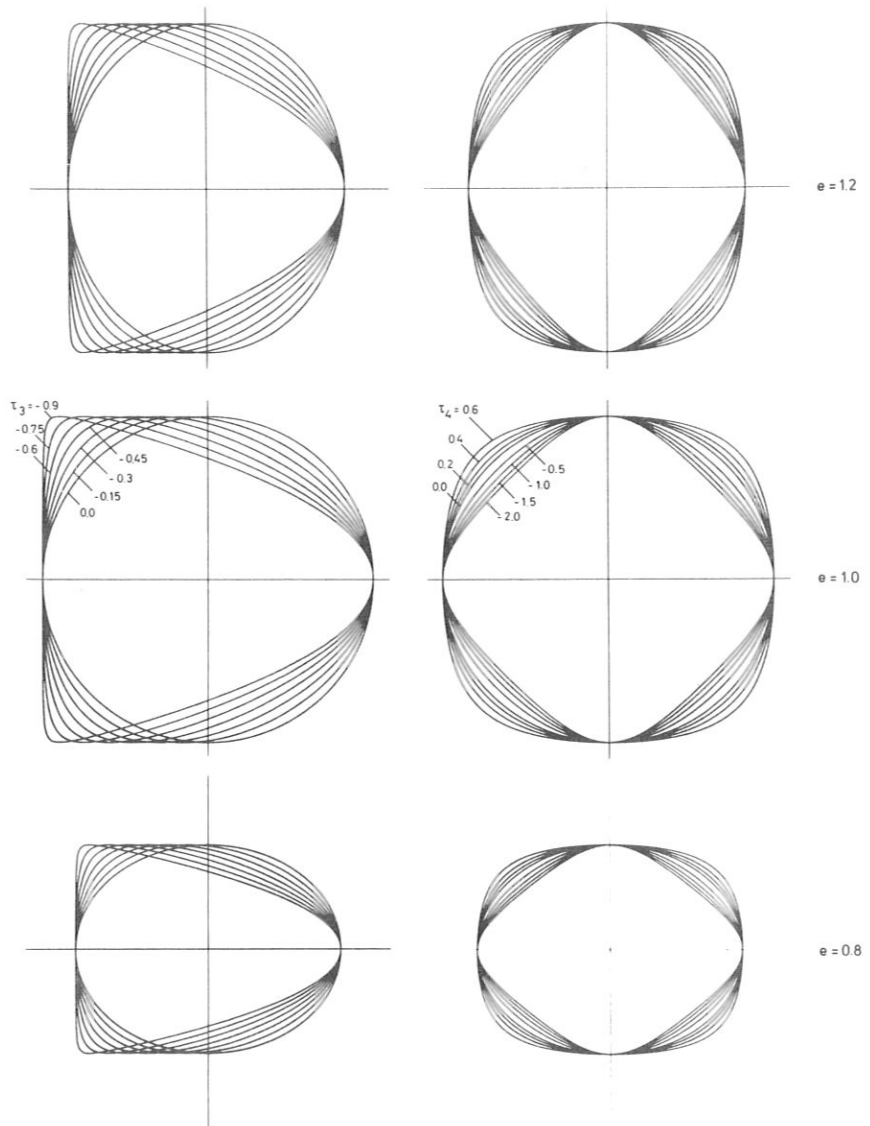


Fig. 2: Typical plasma cross-sections

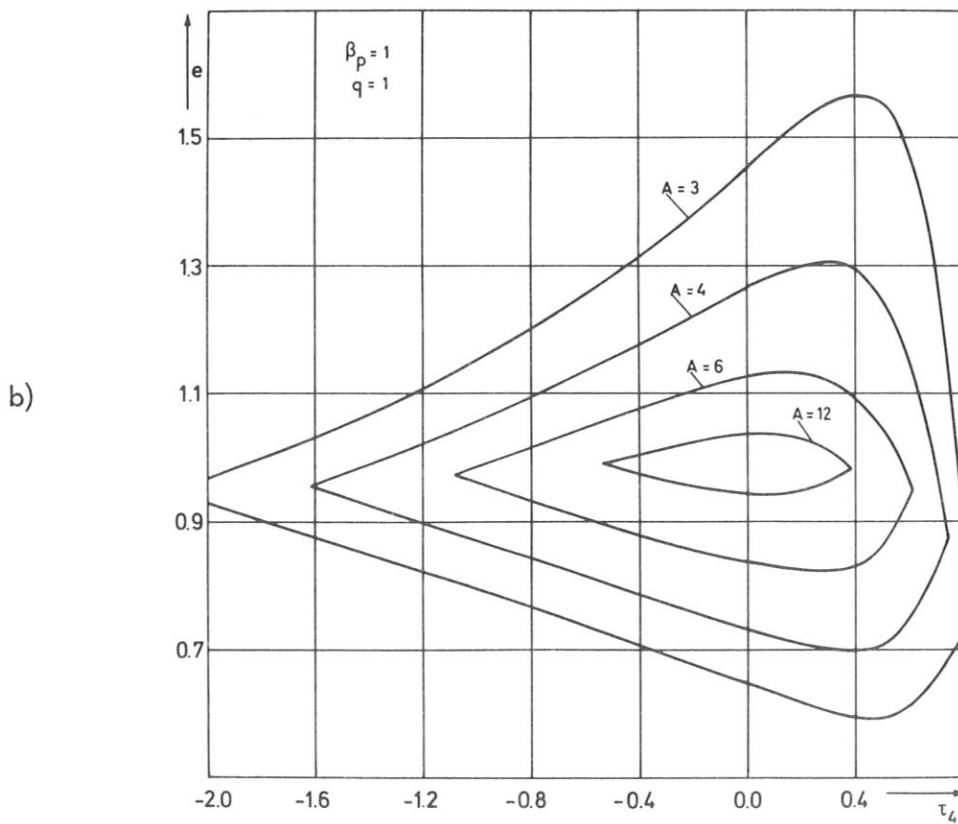
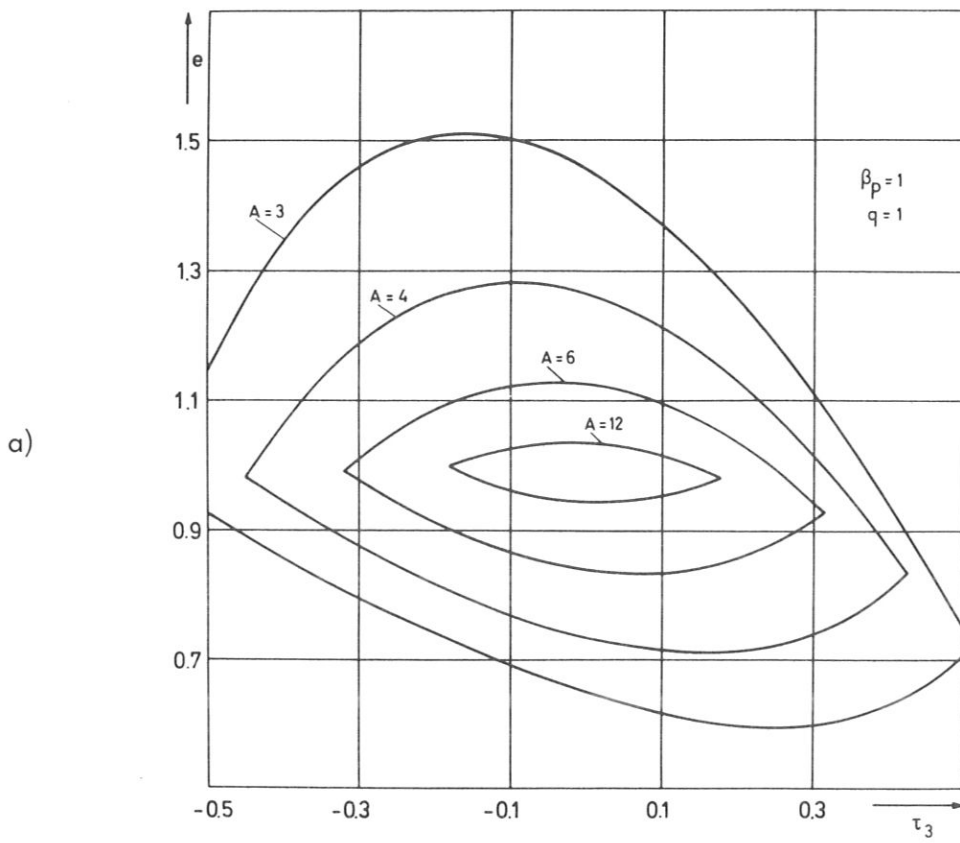


Fig. 3: Stable domains in the τ_3, e plane (Fig. a) and τ_4, e plane (Fig. b) for several values of aspect ratio A .

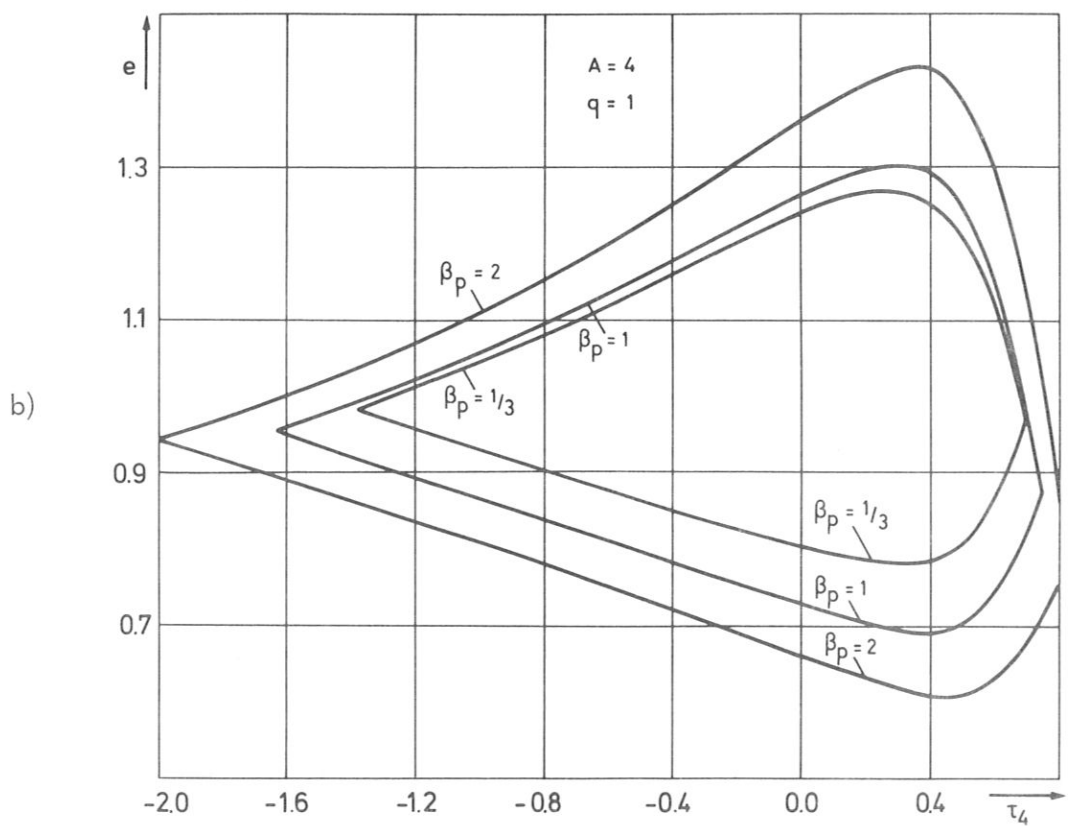
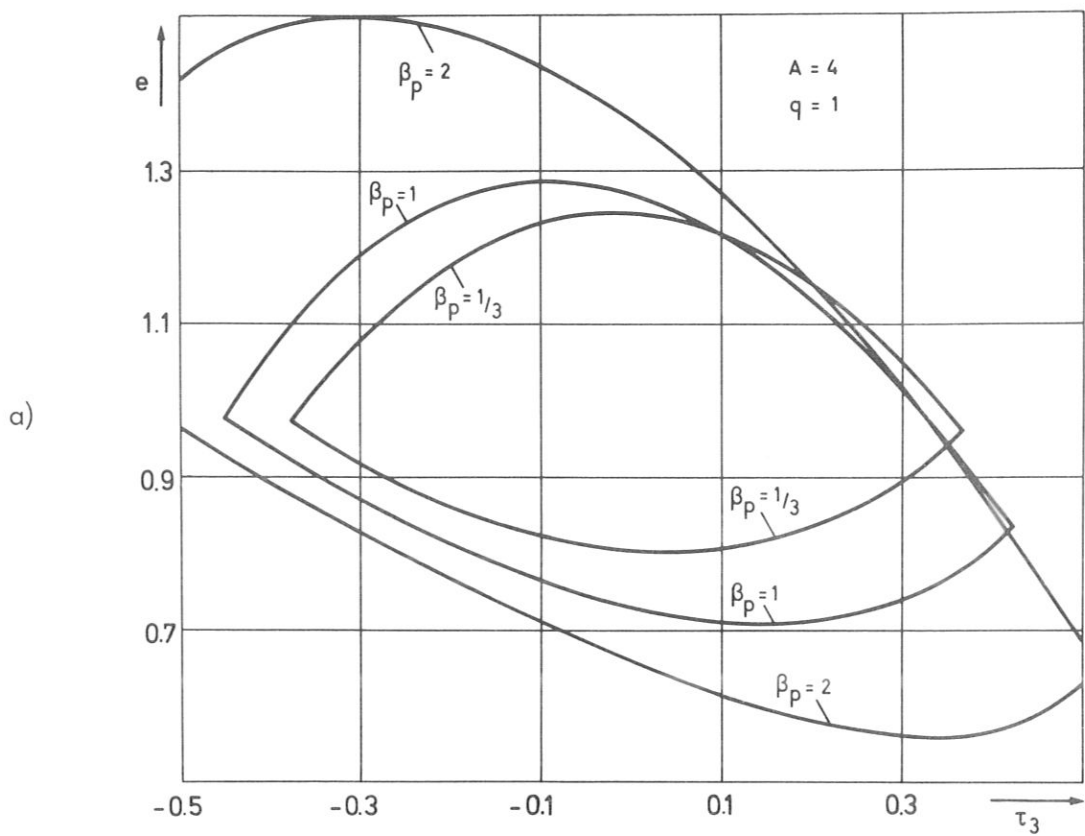
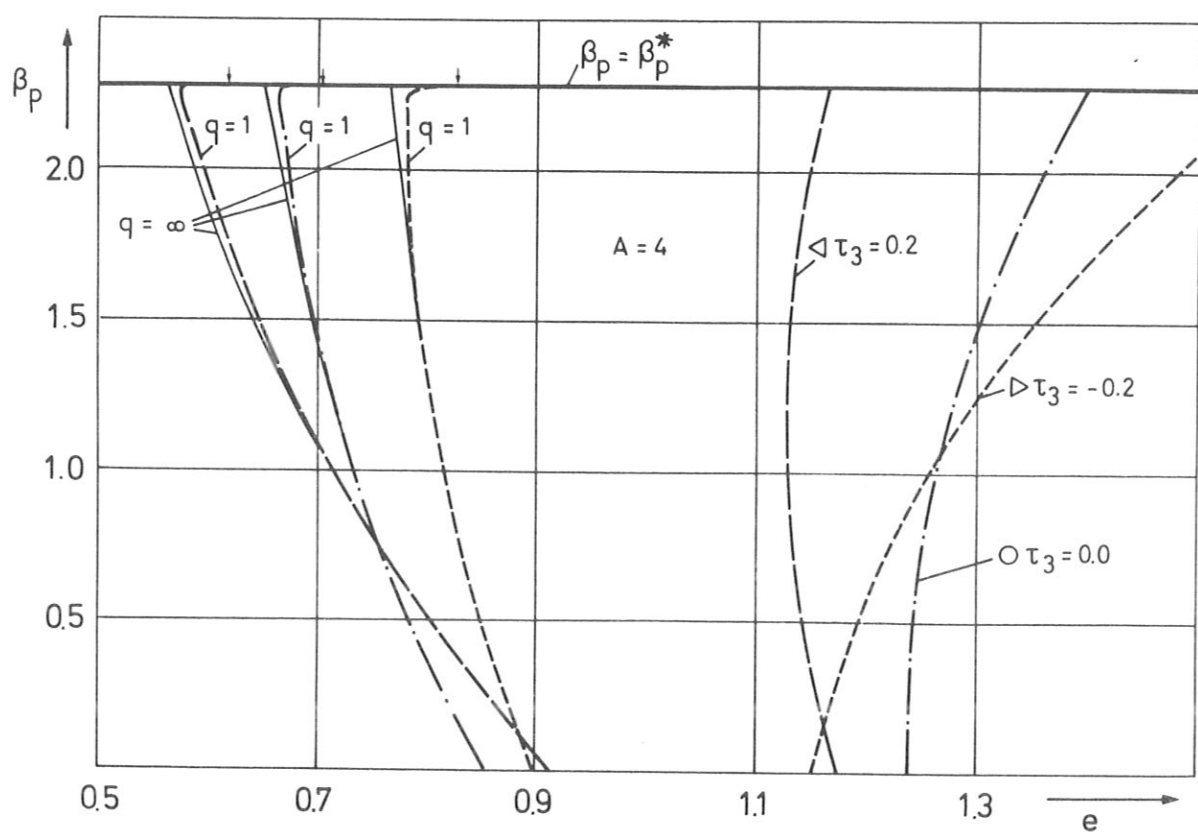


Fig. 4: Stable domains in the τ_3, e plane (Fig. a) and τ_4, e plane (Fig. b) for several values of β_p .

a)



b)

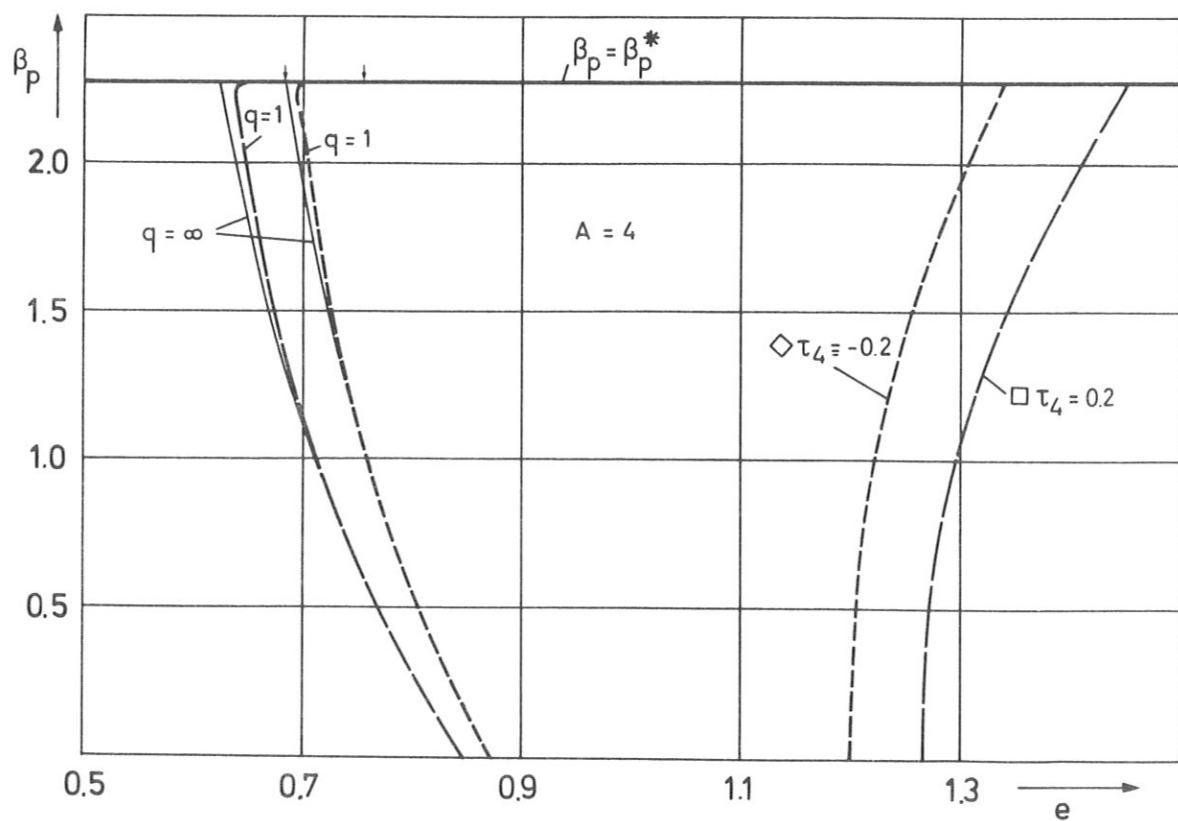


Fig. 5: Stable domains in the e, β_p plane for elliptically, triangularly (Fig. a) and rectangularly (Fig. b) shaped cross-sections; symbols indicate plasma shape.

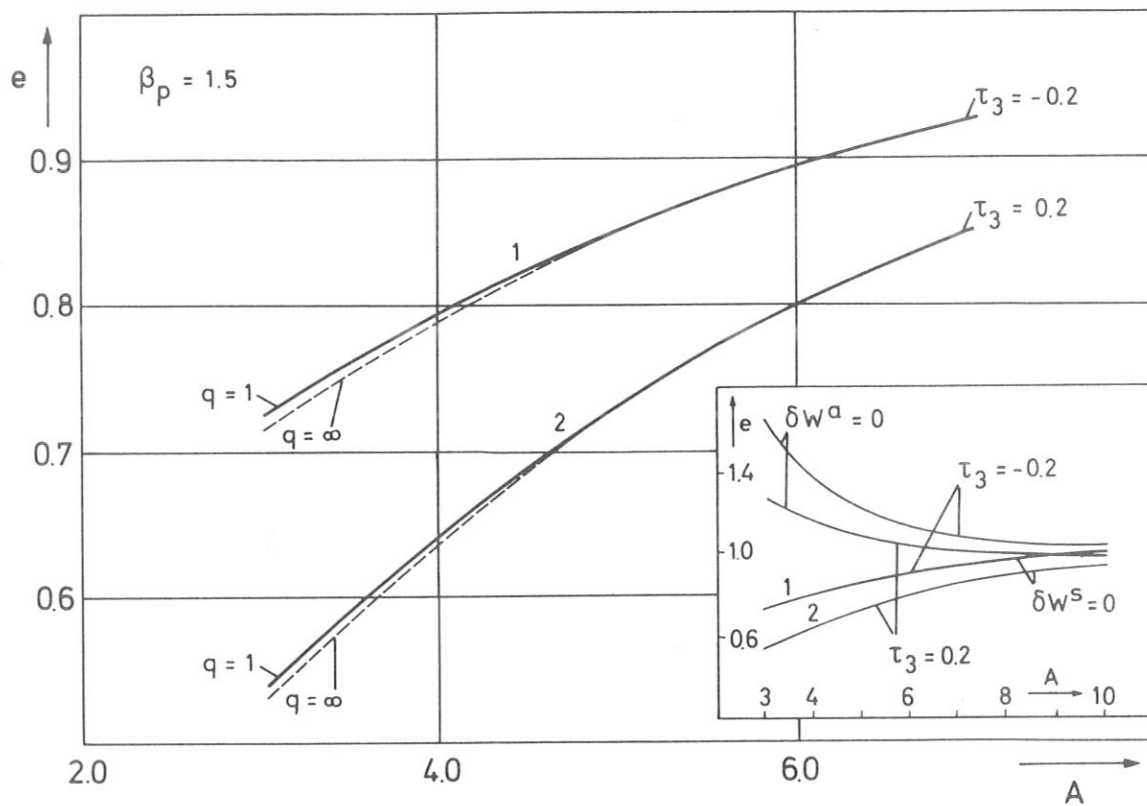


Fig. 6: Stable domains in the A, e plane (insert), and blow-up of the stability boundaries $\delta W^s = 0$.

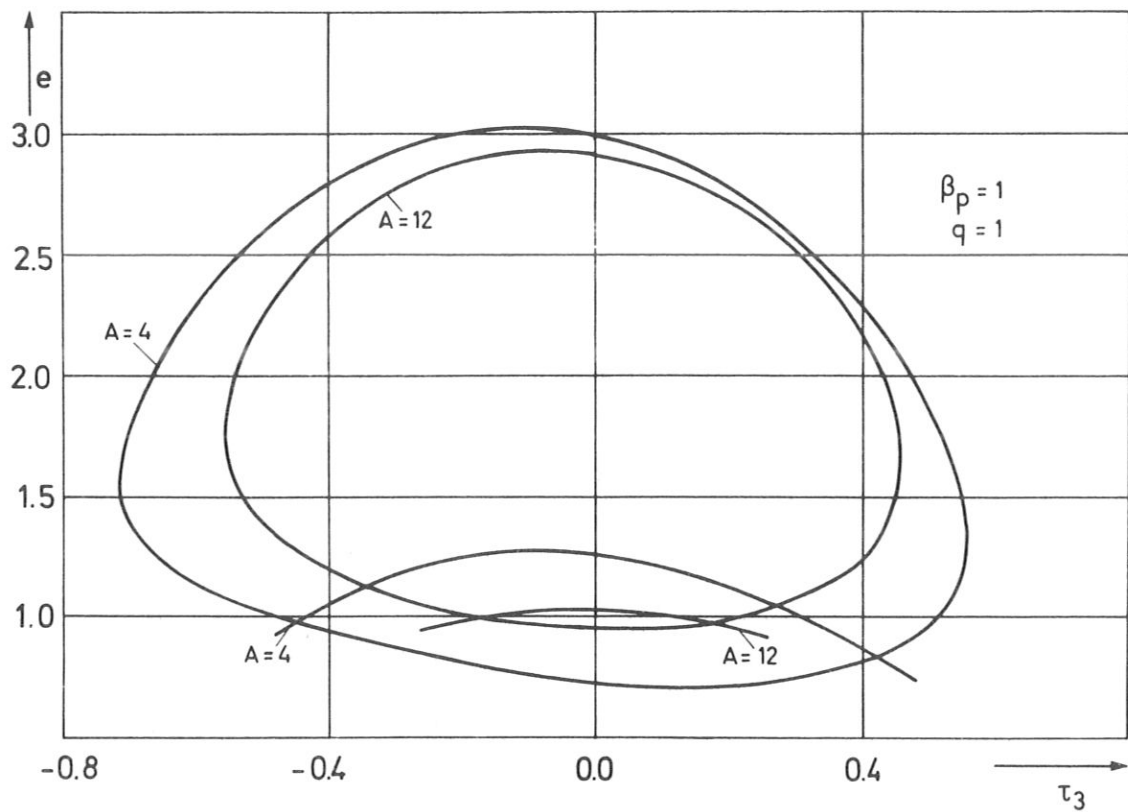
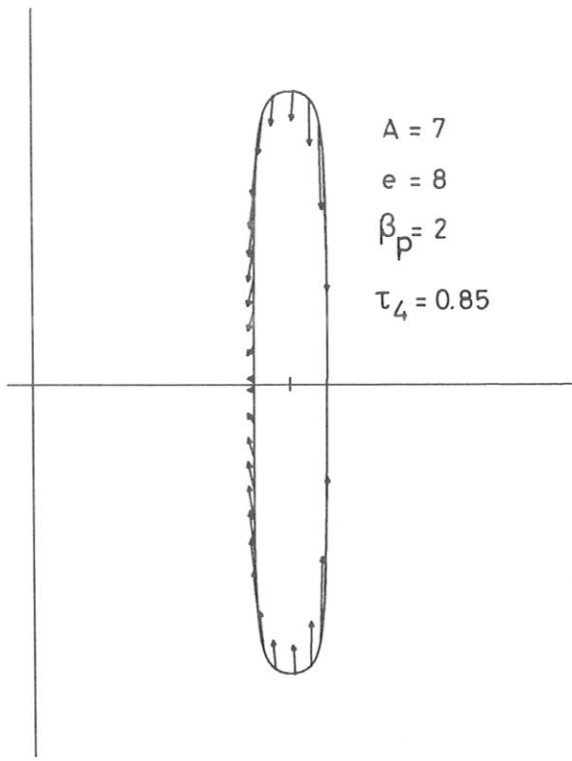
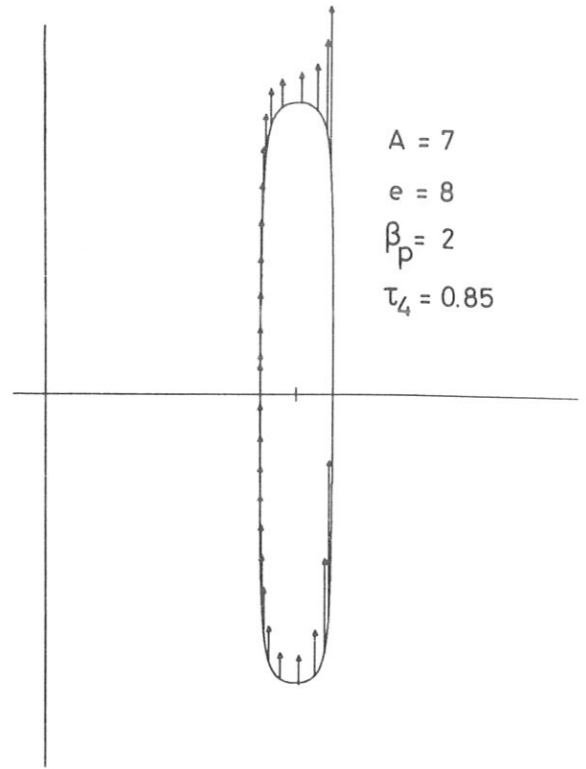


Fig. 7: Continued stability boundaries in the τ_3, e plane.



a)



b)

Fig. 8: Symmetric (Fig. a) and antisymmetric (Fig. b) instabilities in highly elongated tokamaks.

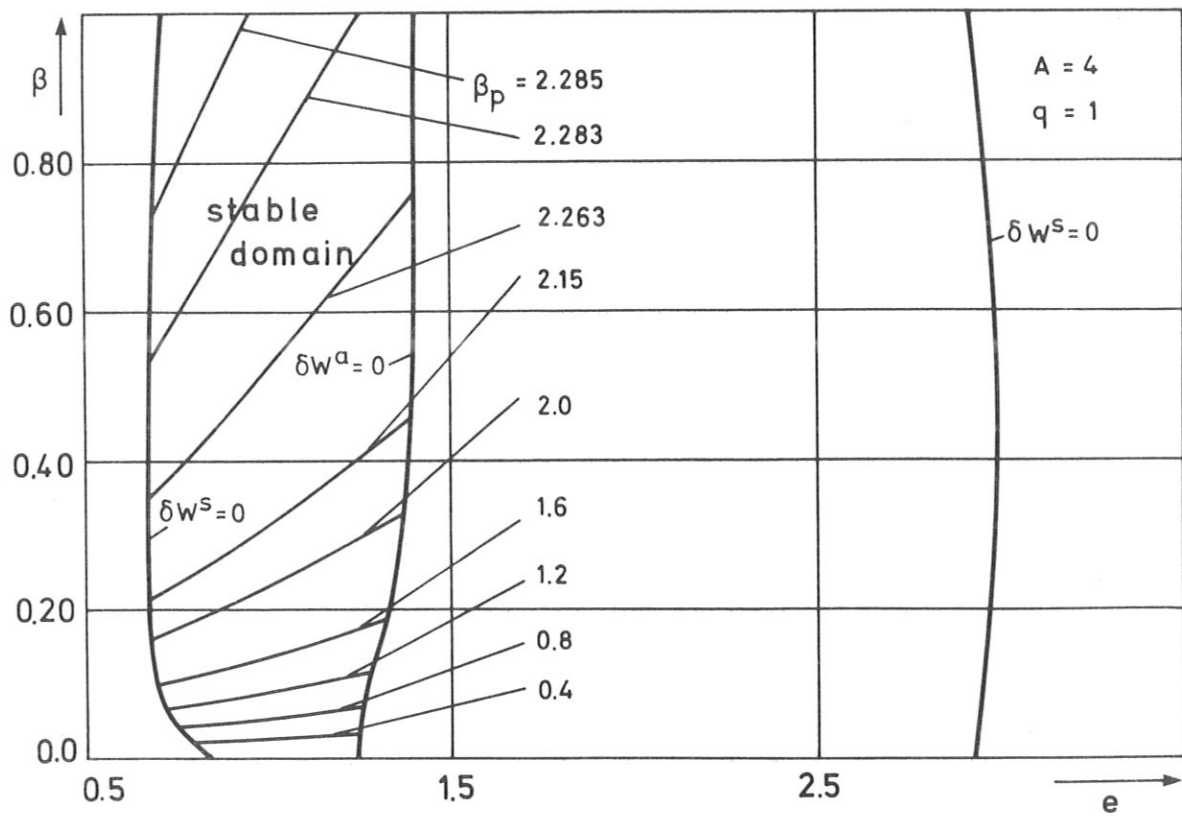


Fig. 9: Stability boundaries for elliptical cross-sections in the e, β plane.

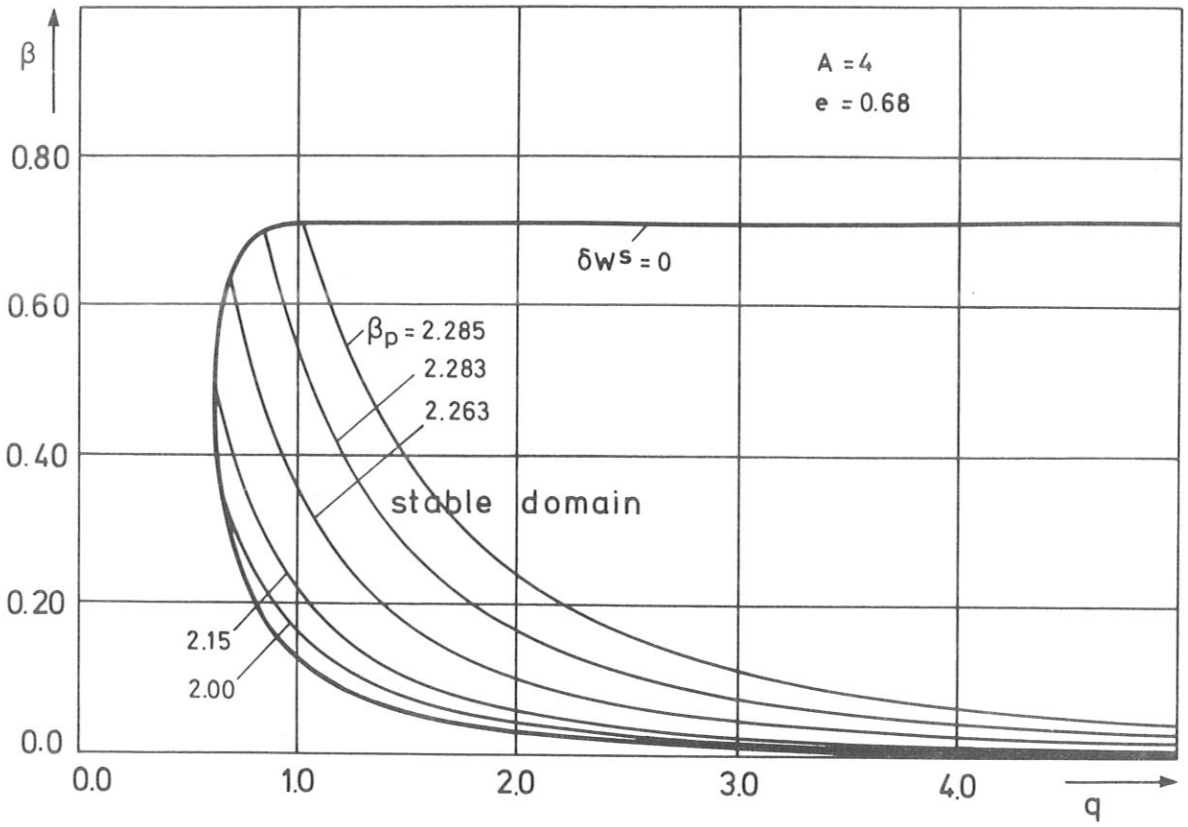


Fig. 10: q dependence of the upper and lower bounds of β for $e = 0.68$.